RPA Phosphorylation in Mitosis Alters DNA Binding and Protein−Protein Interactions†

Gregory G. Oakley,‡,§ Steve M. Patrick,§,|| Jiaqin Yao,‡,⊥ Michael P. Carty,‡,+ John J. Turchi,|| and Kathleen Dixon*,‡

Department of Environmental Health, University of Cincinnati College of Medicine, Cincinnati, Ohio, and Department of Biochemistry and Molecular Biology, Wright State University School of Medicine, Dayton, Ohio

Received July 1, 2002; Revised Manuscript Received January 14, 2003

ABSTRACT: The heterotrimeric DNA-binding protein, replication protein A (RPA), consists of 70-, 34-, and 14-kDa subunits and is involved in maintaining genomic stability by playing key roles in DNA replication, repair, and recombination. RPA participates in these processes through its interaction with other proteins and its strong affinity for single-stranded DNA (ssDNA). RPA-p34 is phosphorylated in a cell-cycle-dependent fashion primarily at Ser-29 and Ser-23, which are consensus sites for Cdc2 cyclin-dependent kinase. By systematically examining RPA-p34 phosphorylation throughout the cell cycle, we have found there are distinct phosphorylated forms of RPA-p34 in different cell-cycle stages. We have isolated and purified a unique phosphorylated form of RPA that is specifically associated with the mitotic phase of the cell cycle. The mitotic form of RPA (m-hRPA) shows no difference in ssDNA binding activity as compared with recombinant RPA (r-hRPA), yet binds less efficiently to double-stranded DNA (dsDNA). These data suggest that mitotic phosphorylation of RPA-p34 inhibits the destabilization of dsDNA by RPA complex, thereby decreasing the binding affinity for dsDNA. The m-hRPA also exhibits altered interactions with certain DNA replication and repair proteins. Using highly purified proteins, m-hRPA exhibited decreased binding to ATM, DNA pol α, and DNA-PK as compared to unphosphorylated recombinant RPA (r-hRPA). Dephosphorylation of m-hRPA was able to restore the interaction with each of these proteins. Interestingly, the interaction of RPA with XPA was not altered by RPA phosphorylation. These data suggest that phosphorylation of RPA-p34 plays an important role in regulating RPA functions in DNA metabolism by altering specific protein−protein interactions.

Eukaryotic RPA[1] is a heterotrimeric single-stranded DNA (ssDNA)-binding protein that has multiple, critical roles in DNA metabolism (*1*−*3*). RPA participates in these diverse functions through its strong affinity for ssDNA and its ability to interact with numerous proteins. There is some evidence that suggests the phosphorylation of RPA may play an important role in regulation of these diverse functions. The p34 subunit of RPA becomes phosphorylated during the normal cell cycle beginning at the onset of S phase, continuing into mitosis, and dephosphorylation occurs in the latter part of mitosis, suggesting a physiological role for RPA-34 phosphorylation in cellular signaling pathways (*4*, *5*). The cell-cycle-dependent phosphorylation events occur primarily at Ser-29 and Ser-23 (*6*), which are consensus sites for cyclin B/p34^{cdc2} kinase (*7*, *8*). In vitro phosphorylation of RPA by cyclin B/p34^{cdc2} yields two forms that migrate slower on polyacrylamide gels than unphosphorylated RPA-p34, a predominant form (Form 2) and a minor form that migrates similar to the mitotic form (Form 3). A serine to alanine mutation of Ser-29 in a synthetic peptide or r-hRPA either inhibited or markedly attenuated phosphorylation by cyclin B/p34^{cdc2} kinase, whereas a serine to alanine mutation of Ser-23 had no effect on phosphorylation levels (*8*, *9*). Ser-29 is the only phosphorylated residue identified in the predominant form, Form 2, suggesting that Ser-29 is the preferred site of phosphorylation by cyclin B/p34^{cdc2} (*8*, *10*, *11*). It has yet to be determined if the minor cyclin B/p34^{cdc2} phosphorylated form (Form 3) is identical to the mitotic form.

In addition to cell-cycle-dependent phosphorylation, RPA-p34 becomes hyperphosphorylated in vivo in response to various genotoxic agents (*11*, *12*). The kinases implicated in this response include DNA-PK_{cs} and ATM (*10*, *13*, *14*). We showed previously that DNA-PK and ATM phosphorylated RPA-p34 at multiple sites in vitro (Ser-11, Ser-12, or Ser-13, Thr-21, Ser-23, Ser-29, and Ser-33), and many of these sites appear to be identical to those phosphorylated in vivo in response to DNA damage (*10*, *14*). Evidence impli-

† This work was supported by Grants R01-NS34782 and P30-ES06096 from the National Institutes of Health and by a research grant from the A-T Children's Project (K.D.) and CA82741 (J.J.T.) from the National Institutes of Health.

* To whom correspondence should be addressed. Tel: (513) 558-1728. Fax: (513) 558-0925. E-mail: Kathleen.Dixon@uc.edu.

‡ University of Cincinnati College of Medicine.

§ Authors contributed equally to this work.

|| Wright State University School of Medicine.

⊥ Current address: Department of Medicinal Chemistry and Pharmacognosy (M/C 781), College of Pharmacy, University of Illinois at Chicago, 833 South Wood Street, Chicago, IL 60612-7231.

+ Current address: Department of Biochemistry, National University of Ireland, Galway, University Road, Galway, Ireland.

[1] Abbreviations: ATR, Rad 3 and ATM related protein; ATM, ataxia telangiectasia mutated; CIP, calf intestinal phosphatase; DNA pol α, DNA polymerase α; DNA-PK, DNA-dependent protein kinase catalytic subunit with Ku70/80 heterodimer; DNA-PK_{cs}, DNA-dependent protein kinase catalytic subunit; m-hRPA, mitotic human replication protein A; r-hRPA, recombinant human replication protein A; hRPA, asynchronous HeLa RPA; ssDNA, single-stranded DNA; dsDNA, double-stranded DNA; XPA, xeroderma pigmentosum group A protein.

10.1021/bi026377u CCC: $25.00
Published on Web 02/19/2003

cating both ATM and DNA-PK_{cs} but not ATR in ionizing radiation (IR)-induced RPA-p34 hyperphosphorylation was obtained using wortmannin and caffeine in vivo (*15*).

The functional effects of phosphorylation of RPA have been examined in a variety of assays; however, a specific role for RPA phosphorylation remains to be elucidated. In cell-free SV40 DNA replication, the presence of phosphorylated RPA or unphosphorylated RPA had no effect on replication efficiency (*16*−*18*). Similarly, phosphorylation of RPA had no effect on NER activity in both HeLa whole cell extracts and NER reconstituted with purified proteins (*17*, *19*). In addition, mutant RPA-p34 lacking N-terminal amino acids 1−33 had no effect on in vitro SV40 replication or DNA repair activity (*9*, *19*). While these data do not rule out possible effects of RPA phosphorylation in vivo, they suggest that phosphorylation of RPA does not directly affect DNA replication or NER in cell-free systems.

As for checkpoint activation, the finding that overexpression of the ATM kinase domain in A-T cells failed to phosphorylate RPA yet corrected the radiosensitivity of these cells suggested phosphorylation of RPA-p34 can be dissociated from checkpoint activation (*20*). Similarly, UCN-01 (a protein kinase C, cyclin-dependent kinase and Chk1 inhibitor), which abrogates the S and G_2 checkpoints, had no effect on IR-induced RPA-p34 phosphorylation in HeLa cells providing additional evidence that RPA phosphorylation can be dissociated from checkpoint activation (*15*).

Conversely, other experimental evidence suggests that RPA phosphorylation may play a regulatory role in DNA replication. First, we have previously shown that UV-induced RPA hyperphosphorylation occurs concomitantly with a loss of SV40 replication efficiency, but replication efficiency was restored to the level of untreated cells with the addition of unphosphorylated RPA (*11*). Liu et al. observed a similar inactivation of SV40 replication by adozelesin and rescue with unphosphorylated RPA (*21*). Further evidence that RPA hyperphosphorylation is related to DNA synthesis inhibition is shown by camptothecin-induced DNA inhibition coinciding with RPA hyperphosphorylation. Furthermore, UCN-01 treatment blocked camptothecin-induced RPA-p34 phosphorylation in vivo (*22*). These observations allude to a regulatory role for RPA phosphorylation in DNA replication in response to DNA damage.

RPA is known to interact specifically with numerous DNA replication, recombination, and repair proteins including DNA pol α and SV40 large tumor antigen; transcription factors VP16 and GAL4; DNA repair proteins XPA, DDB, XPF, and XPG; the Rad52 epistasis group; DNA helicases, Blooms (BLM) and Werners (WRN) proteins; and proteins involved in cell cycle control and/or DNA damage response such as p53, cdc2, and DNA-PK (*22*−*31*). The direct physical association between RPA and other proteins is primarily via the N-terminus of RPA-p70 with some contribution from the C-terminus, although XPA, Rad52, and Rad51 interact with RPA-p34 in addition to the N-terminus of RPA-p70 (*24*, *31*, *32*). The association between p53 and RPA is disrupted following UV damage, providing indirect evidence that RPA-p34 phosphorylation alters the ability of RPA to interact with proteins (*33*).

To investigate the role of RPA-p34 phosphorylation in protein function, we have purified a cell-cycle specific phosphorylated form of RPA, m-hRPA, and examined DNA binding activity and protein−protein interactions. Here, we demonstrate that phosphorylated RPA has a 4−6-fold decrease in binding affinity for undamaged and cisplatin-damaged dsDNA, yet exhibits similar ssDNA binding activity as compared to unphosphorylated r-hRPA. In addition, the phosphorylated form of RPA exhibited decreased protein−protein interactions with ATM, DNA pol α, and DNA-PK. In contrast, RPA phosphorylation did not alter interaction with the DNA repair protein XPA. Based on these observations, we propose that phosphorylation of RPA-p34 plays a role in regulating cellular DNA replication and DNA repair functions by altering protein−protein and protein−DNA interactions.

MATERIALS AND METHODS

Cell Culture. HeLa cells were grown in Dulbecco's Minimal Essential medium (DMEM) containing 10% fetal bovine serum (FBS) and 1% penicillin-streptomycin, at 37 °C and 5% CO_2.

Flow Cytometry and Cell Elutriation. HeLa cells were fixed at a density of 2×10^6/mL overnight in 70% ethanol at −20 °C. The following day, the cells were sedimented at 300*g* in a swinging bucket centrifuge for 10 min at 4 °C. The cells were resuspended in the propidium iodide master mix [phosphate buffered saline (PBS) containing 1 μg/mL RNAse A, 1.6 μg/mL propidium iodide] and incubated at 37 °C for 1 h. The cells were washed twice and resuspended with PBS containing propidium iodide (1.6 μg/mL) at a density of 1×10^6/mL. The cells were filtered through a 40 μm nylon mesh filter immediately prior to sorting. The cells were elutriated using a FACS Vantage SE cell sorter (Bectin Dickinson, San Diego, CA).

DNA Synthesis Assay. Thymidine incorporation was assayed essentially as described previously (*14*). Briefly, cells were pre-labeled with 0.01 μCi/mL ^{14}C-thymidine (Perkin-Elmer, Inc., Boston, MA) for 24 h at 37 °C. After incubation in fresh medium for 1 h, cells were treated with nocodazole (0.3 μM). The rate of DNA synthesis after release from nocodazole treatment was measured by ^{3}H-thymidine incorporation during a 30 min pulse with 10 μCi/mL ^{3}H-thymidine (Perkin-Elmer, Inc., Boston, MA). After labeling with ^{14}C-thymidine and ^{3}H-thymidine, cells were washed with PBS twice and lysed with 500 μL of 0.2 M NaOH. Triplicate samples (150 μL each) were collected onto Whatman #3 circles (Whatman International, Maidstone, England) and rinsed with 5% trichloroacetic acid and then 100% ethanol. The radioactivity of each sample was counted by dual-label liquid scintillation, and the ratio of ^{3}H/^{14}C reflected the DNA synthesis activity.

Purification of RPA, XPA, DNA pol α, and DNA-PK. HeLa cells grown in flasks were treated with the microtubule inhibitor nocodazole (0.3 μM, Sigma, St. Louis, MO) for 17 h (*4*). Mitotic cells were separated from the interphase cells by gently shaking off the mitotic cells. Hypotonic extracts were prepared as described previously (*11*). Briefly, the cells were washed with PBS and extracted in 20 mM HEPES (pH 7.5), 5 mM KCl, 1.5 mM $MgCl_2$, 1 mM dithiothreitol (DTT), 25 μM bromotetramisole oxalate, 5 μM cantharidin, and 5 nM microcystin LR followed by clarification by centrifugation at 15 000*g* for 10 min. The protein concentration of the cell extracts was estimated using

the BCA protein assay (Pierce, Rockford, IL). The hRPA form of RPA was purified from asynchronously growing HeLa cells. The r-hRPA protein was expressed and purified from *Escherichia coli* BL21 (DE3) cells transformed with p11d-tRPA vector (a gift from Dr. Marc Wold, University of Iowa, Iowa City, IA) as described previously (*34*). The m-hRPA and hRPA forms of RPA were purified using the same chromatographic steps as with r-hRPA (*34*, *35*). Briefly, the extracts were loaded onto a 20-mL Affi-gel blue column equilibrated in HI buffer (30 mM HEPES, pH 7.8, 0.01% NP-40, 0.25 mM EDTA, 1 mM DTT, and 0.25% inositol) supplemented with 0.1 M KCl. The column was washed with HI buffer containing 0.8 M KCl followed by HI buffer supplemented with 0.5 M NaSCN. The protein was eluted from the column using HI buffer supplemented with 1.5 M NaSCN, and the peak protein based on absorbance at 280 nm was directly loaded onto a 2-mL hydroxylapatite column equilibrated in HI buffer. The column was washed with HI buffer, and RPA was eluted with HI buffer containing 100 mM KP_i. The peak protein was loaded directly onto a 2-mL Q-Sepharose column equilibrated in HI buffer and washed with HI buffer supplemented with 0.1 M KCl. RPA was eluted with HI buffer using a linear gradient from 0.1 to 1 M KCl. The peak fractions based on SDS gel analysis of m-hRPA were pooled and dialyzed in HI buffer.

XPA was expressed as a [His]6-XPA fusion protein in Sf-21 insect cells following infection with a recombinant baculovirus. The protein was purified using metal chelate affinity chromatography as previously described (*36*). DNA pol α was purified from calf thymus by immunoaffinity chromatography according to Nasheuer and Grosse (*37*). DNA-PK was purified from HeLa cells using traditional column chromatography as previously described (*38*).

Stopped-Flow Kinetic Experiments and Data Analysis. Stopped-flow kinetic traces and data analysis were performed as previously described (*35*). Briefly, the traces were obtained using a SX.18MV stopped-flow reaction analyzer (Applied Photophysics). Reactions were performed in buffer containing 20 mM HEPES (pH 7.8), 2 mM DTT, 0.001% NP-40, and 50 mM NaCl. Constant RPA (6.25 nM final concentration) and varying DNA concentrations (62.5−125 nM) starting at a 10-fold excess of DNA were used to achieve pseudo-first-order kinetics (*35*). The trace shown represents the average of 10 individual shots. The observed rate k_{obs} was calculated using Pro-K software (Applied Photophysics), and the rate constants were determined using linear regression analysis (SigmaPlot, Jandel). The slope of the line is the bimolecular association rate, k_{on}, and the *y* intercept is the rate of dissociation, k_{off} (*35*). The large k_{obs} values for each DNA concentration and the slow dissociation results in large errors associated with the k_{off} determinations and thus a negative *y* intercept value. These data are consistent with r-hRPA; thus, the k_{off} value was not determined for the m-hRPA.

Electrophoretic Mobility Shift Assay (EMSA). EMSAs were performed as previously described (*34*). Briefly, reactions were carried out in 20 mM HEPES (pH 7.8), 2 mM DTT, 0.001% NP-40, 50 mM NaCl, 50 μg/mL bovine serum albumin, and 50 fmol of ssDNA or 20 fmol of dsDNA. The ssDNA substrate was a dT_{30} DNA substrate as used previously (*35*). The 30-bp dsDNA substrates with and without a single, centrally located 1,2 d(GpG) cisplatin adduct were prepared as previously described to ensure minimal single-strand DNA contamination (*34*, *35*). Each reaction in the ssDNA EMSAs contained 200 ng of the RPA-p34 antibody to supershift the RPA-DNA band, which resulted in a cleaner band shift. Reaction products were electrophoresed on a 4% native polyacrylamide gel. The gels were visualized and quantified by phosphorimager analysis (Molecular Dynamics, Sunnyvale, CA).

Immunoblotting. For Western immunoblots, samples were solubilized in Laemmli sample loading buffer, placed at 100 °C for 5 min, and then separated on 13% denaturing SDS−polyacrylamide gels (monomer-to-crosslinker ratio 37.5:1) with a 4% stacking gel using the Laemmli buffer system. Proteins were transferred to Immobilon-P polyvinyl-divinyl fluoride transfer (PVDF) membranes (Millipore Corp., Bedford, MA) in 50 mM 3-(cyclohexylamino)propanesulfonic acid (pH 11.0) and 10% methanol at 500 mA for 1 h (*39*). Membranes were blocked for 15 min in blocking buffer (2% nonfat dry milk, 0.1% Tween 20 in PBS) and then incubated with anti-RPA-p34 monoclonal antibody or isotype control for RPA (1:5000; Neomarkers, Fremont, CA) for 15−20 min at 37 °C. After washing four times with 0.1% Tween 20 in PBS, membranes were incubated with a 1:3000 dilution of horseradish peroxidase-linked goat anti-mouse secondary antibody for 15 min. Membranes were washed as described and visualized using chemiluminescent detection.

Immunoprecipitation. For co-immunoprecipitation assays, 100 ng of r-hRPA or m-hRPA were incubated with either 500 ng of purified XPA (*36*), ATM (*14*), DNA-PK (*38*), or DNA pol α (*37*) in PBS containing 0.05% NP-40 for 30 min with end-over-end mixing at 4 °C. Following the addition of 0.5−3.0 μg of anti-XPA, ATM, DNA-PK, or DNA pol α antibody, the immunoprecipitates were incubated overnight at 4 °C. After the addition of 30 μL of protein G-agarose (Gibco-BRL) for 2 h, the immunoprecipitates were separated from the supernatant by centrifugation at 5000*g* for 5 min. The immunoprecipitates were washed three times with 0.01% NP-40- PBS, resuspended in 1X Laemmli gel loading buffer, and separated on a 13% SDS−polyacrylamide gel.

RESULTS

G2/M Phase of the Cell Cycle Is Required for Mitotic Specific Phosphorylated Form of RPA-p34 (m-hRPA). In normal cycling HeLa cells, RPA-p34 exists in three different forms that can be resolved by SDS−PAGE. One of these forms, Form 3, is the predominant form observed following nocodazole-induced cell-cycle arrest in mitosis. The fact that the majority of RPA-p34 is phosphorylated in one specific form may be attributed to the presence of nocodazole rather than a specific mitotic form of the protein. To determine if the phosphorylated Form 3 is specific to mitosis, exponentially growing HeLa cells were treated with nocodazole for 17 h and released. Following release, cell cycle progression through G_1, S, and back into G_2/M phase was monitored by ^{3}H thymidine incorporation (Figure 1A). Peak incorporation during S-phase occurred approximately 15 h post-release (Figure 1A), confirming the release from the nocodazole-induced cell-cycle block. The different forms of RPA-p34 were monitored as cells progress throughout the cell cycle after removal of nocodazole. In addition, nocodazole-blocked

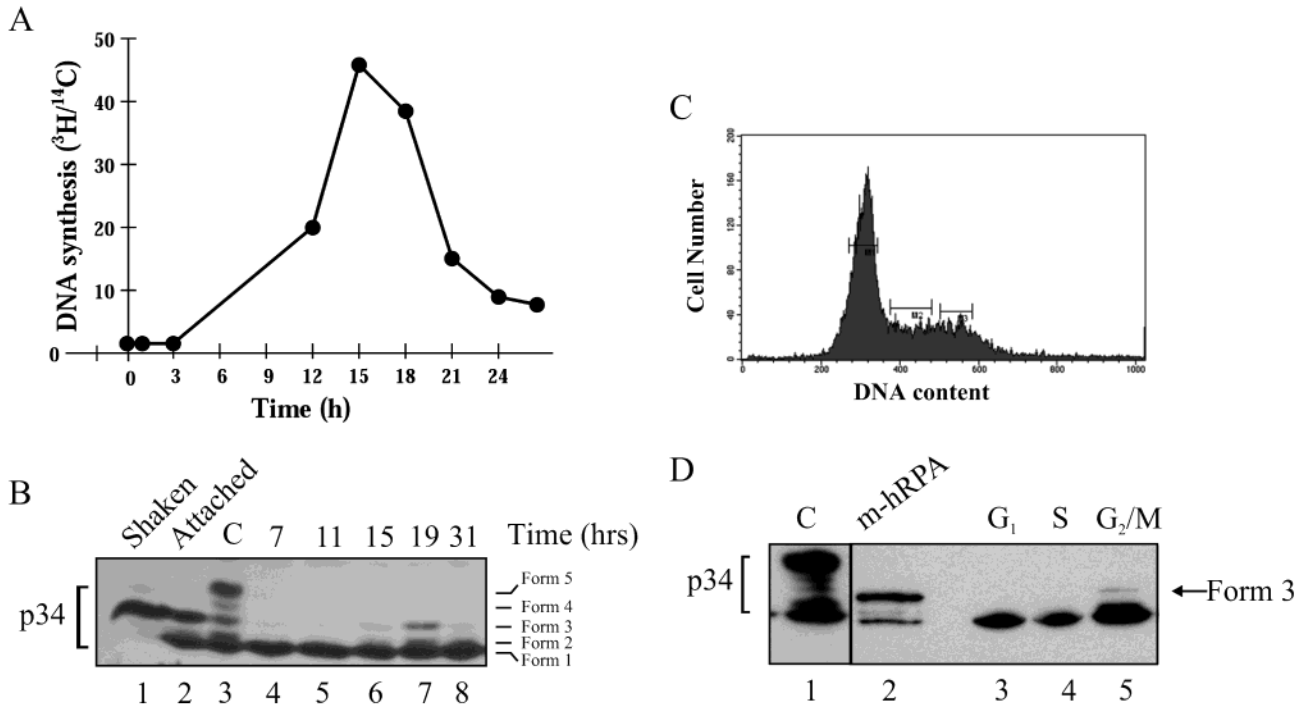

FIGURE 1: G2/M phase of the cell cycle is required to regenerate the mitotic specific phosphorylated form of RPA-p34 (m-hRPA) following cell synchronization with nocodazole. (A) Time course of DNA synthesis following nocodazole release. The rate of DNA synthesis after release from nocodazole treatment (0.3 μM) was measured as ^{3}H-thymidine incorporation during a 30 min pulse with 10 μCi/mL ^{3}H-thymidine. Cells were pre-labeled with 0.01 μCi/mL ^{14}C-thymidine for 24 h at 37 °C followed by ^{3}H-thymidine pulse labeling. After labeling, cells were washed with PBS twice and lysed with 500 μL of 0.2 M NaOH per dish. The radioactivity of each sample was counted by dual-label liquid scintillation, and the ratio of ^{3}H/^{14}C reflected the DNA synthesis activity. (B) Time course of RPA-p34 phosphorylation following release from nocodazole treatment (lanes 4−8). Mitotic cells were shaken from the dish after nocodazole treatment (lane 1) and compared to attached cells (lane 2). Following preparation of hypotonic extracts, RPA-p34 was visualized by immunoblotting with anti-RPA-p34 antibody and chemiluminescent detection. Phosphorylation causes a slower migration on the gel; at least five different forms of the p34 subunit of RPA can be visualized; Form 1 is unphosphorylated RPA-p34, Forms 2 and 3 are cell cycle dependent phosphorylated forms, and Form 5 is the DNA damage-induced hyperphosphorylated form as shown in the positive control (lane 3, long-term aphidicolin treatment, 6 μM at 24 h). (C) FACS analysis of cells from an asynchronous growing HeLa cell population. (D) Immunoblot analysis of RPA-p34 from cell fractions corresponding to G_1, S, and G_2/M cell-cycle populations (lanes 3−5). DNA damage-induced hyperphosphorylated form as shown in the positive control (lane 1, UVC 30 J/m^2 at 8 h). The purified m-hRPA is in lane 2. Cell lysates were prepared from asynchronously growing HeLa cells, and the p34 subunit of RPA was detected with anti-RPA-p34 monoclonal antibody (1:5000).

cells were processed by gently shaking off loosely attached mitotic cells (Figure 1B, lane 1); the remaining attached cells were also processed for Western blot analysis (lane 2). An extract (lane 3) from cells subject to DNA damage [long-term aphidicolin treatment, 6 μM at 24 h (*40*)] is also included as a control to delineate the various forms of RPA-p34. Form 1 represents unphosphorylated and perhaps some partially phosphorylated forms of RPA-p34, Forms 2 and 3 are cell-cycle-dependent phosphorylated forms, and Form 5 is the DNA damage-induced hyperphosphorylated form. In nocodazole-blocked cells that were shaken off the dish, Form 3 is the predominant form of RPA-p34 and also represents a large portion of the RPA-p34 in cells remaining attached to the plate. At 7 h after release, in the G_1 phase of the cell cycle, the protein becomes largely dephosphorylated (Figure 1B, lane 4). As cells progress through S-phase, Form 2 was observed (Figure 1B, lane 6). Form 3 appeared most strongly at 19 h after release from nocodazole as the cells traversed G_2 and into mitosis, providing further evidence that Form 3 represents a mitotic form of RPA-p34. To further verify this was a cell-cycle specific phosphorylated form of RPA-p34 and not due to the presence of the microtubule-disrupting drug nocodazole, asynchronous exponentially growing HeLa cells were sorted by counterflow centrifugal elutriation and FACS analysis. With this method, cell populations were fractionated by means of size, density, and DNA content, and cell lysates were prepared from fractions corresponding to discrete cell-cycle phase-specific populations. Immunoblot analysis revealed that the majority of the protein present in G_1 and S-phase cells was in Forms 1 and 2 (Figure 1D, lanes 3 and 4), while as cells progress through S into the G_2/M phase the appearance of a form of the protein with the same gel mobility as that observed in nocodazole-arrested mitotic cell was present (Figure 1D, lane 5). Although the proportion of Form 3 appears negligible in the G_2/M fraction, this is likely due to phosphatase activity in the collected cells. Also, there are likely to be more G_2 than M phase cells in the G_2/M fraction, reducing the contribution of m-hRPA to the total observed. These results are consistent with the conclusion that Form 3 of RPA-p34 is the mitotic form of the protein, and the presence of this form after nocodazole treatment is not attributable simply to the presence of the drug. This suggests a strict regulation of the phosphorylation of this protein during cell cycle progression.

Purification of m-hRPA. To investigate the effect of mitotic RPA-p34 phosphorylation on DNA binding and protein−protein interaction, we have used conventional biochemical techniques to purify phosphorylated RPA from nocodazole treated HeLa cells. Initial fractionation of cellular extracts was accomplished on an Affi-Gel blue column as described

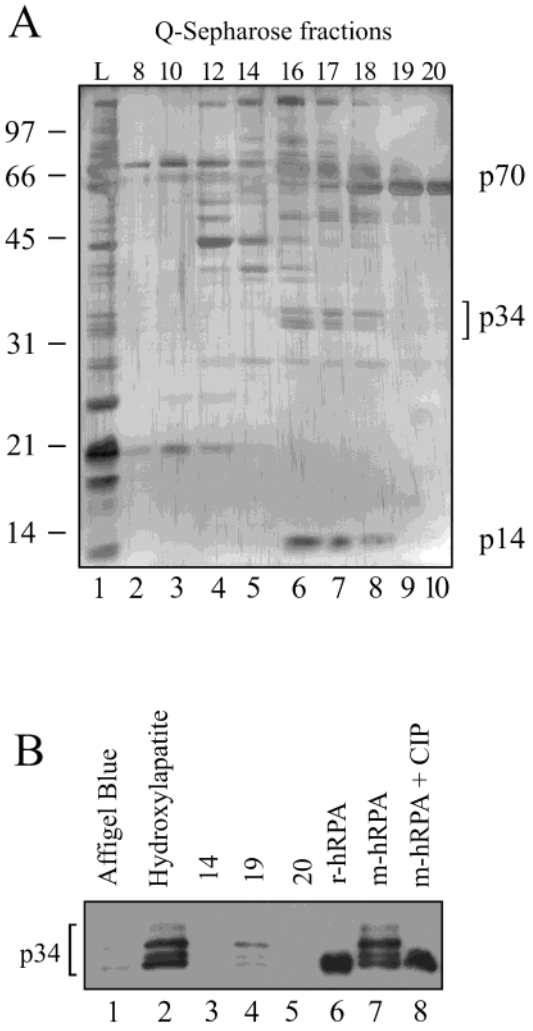

FIGURE 2: Purification of m-hRPA. (A) Protein fractions were visualized on a 13% SDS−polyacrylamide gel by silver staining. Lanes contain an equal volume from the hydroxylapatite column (L; lane 1) and fractions from the Mono-Q column (lanes 2−10). The positions of the subunits of RPA are indicated (p70, p34, and p14). (B) Immunoblot of the Affi-gel blue peak fractions; hydroxylapatite pooled fractions; Mono-Q fractions 14, 19, and 20 r-hRPA; Mono-Q pooled fractions 15−18 (m-hRPA; lane 7); and Mono-Q pooled fractions with 40 units of calf intestinal phosphatase (lane 8).

in the Materials and Methods. Further purification was achieved with hydroxylapatite and Q-Sepharose columns under the same conditions as for purification of r-hRPA (see Materials and Methods). A silver stained SDS−PAGE gel of fractions from the purification of m-hRPA is shown in Figure 2A. R-hRPA was used as a marker to verify the position of m-hRPA (not shown). The hydroxylapatite pool that was loaded on the Q-Sepharose column is in lane 1 followed by fractions from the gradient elution from the Q-Sepharose column. The RPA protein is concentrated in fractions 16−18 (Figure 2A, lanes 6−8) from the Q-Sepharose column, and the p34 subunit appears to have three distinct bands or phosphorylated forms (Forms 1−3). These fractions were pooled as m-hRPA. The final pool and additional fractions were analyzed by SDS−PAGE and the Western immunoblotting (Figure 2B). We estimated that Form 3 represents 40% of the RPA-p34 present in the pool. We verified that the slower migrating forms of RPA-p34 represent phosphorylated forms of the protein as treatment of the protein with calf intestinal phosphatase (CIP) resulted in a loss of these slower migrating species of RPA (Figure 2B, lane 8) generating a band that migrates similarly to the r-hRPA (Form 1). Although band 1 runs with the same mobility as the r-hRPA protein, it does not appear to represent unphosphorylated RPA in the m-hRPA purification product. Two-dimensional gel analysis suggests that all forms within the mitotic pool of protein are phosphorylated, but Form 1 cannot be separated into distinct phosphorylated forms on one-dimensional SDS gels (data not shown). Form 2 most likely represents one or two phosphates on the RPA-p34 subunit, while Forms 3 and 4 most likely represent a p34 subunit with multiple phosphates (*10*). Phosphatase inhibitors are required in the purification buffers to obtain purified phosphorylated RPA.

m-hRPA Has Similar ssDNA Binding Activity as r-hRPA. The DNA binding activity of RPA is crucial for many DNA metabolic processes. Whether RPA phosphorylation plays a role in DNA binding and ultimately in RPA regulation has not been definitively addressed. Thus, having purified m-hRPA, we sought to characterize the DNA binding activities of the phosphorylated RPA versus the unphosphorylated r-hRPA protein. Electrophoretic mobility shift analyses (EMSAs) were performed using a dT_{30} ssDNA substrate (Figure 3A). Increasing concentrations of either m-hRPA or r-hRPA were titrated into reactions, and bound RPA-DNA was observed. RPA-p34 monoclonal antibody (125 ng) was added to each reaction to super-shift the RPA−DNA complex, resulting in a cleaner band shift. The quantification of the EMSA (Figure 3B) reveals no difference in ssDNA binding activity between m-hRPA or r-hRPA. The equilibrium binding experiment was also performed in the absence of RPA antibody, and the relative binding activity of phosphorylated and unphosphorylated RPA was similar to that shown in Figure 3 (data not shown). Thus, phosphorylation of the p34 subunit appears to have no measurable effect on RPA ability to bind a dT_{30} ssDNA substrate.

To confirm the EMSA results, stopped-flow kinetic analysis was performed using the same dT_{30} DNA substrate as used in the EMSA experiments and in a previous study with r-hRPA (*35*). As RPA binds DNA, the intrinsic fluorescence of the protein is quenched, and this quenching can be monitored over time to generate observed rates of quenching, k_{obs}, values (*35*). Figure 4A is a kinetic trace of m-hRPA mixed with dT_{30} DNA. Time zero represents the relative fluorescence of the m-hRPA in the absence of DNA and upon mixing with the DNA substrate, a quenching of the fluorescence is observed. The quenching of constant RPA (6.25 nM) was monitored over time with varying DNA concentrations (62.5−125 nM). Each trace was fit to a single-exponential decay (thick line), and the residual values were presented in the panel below the trace. The resulting k_{obs} values were plotted versus DNA concentration (Figure 4B). The results revealed a linear relationship with the slope being the bimolecular association rate, k_{on}, and the *y* intercept equal to the k_{off} (*35*). The k_{on} of the m-hRPA for dT_{30} ssDNA was 2.46 ± 0.435 nM^{-1} s^{-1}, while the r-hRPA protein has a k_{on} of 2.14 ± 0.08 nM^{-1} s^{-1} (*35*). The *y* intercept value for the m-hRPA resulted in a negative value suggesting a slow dissociation, consistent with that observed with r-hRPA (*35*). The k_{on} values are indistinguishable, and the consistently slow dissociation is consistent with the EMSA in that there is no

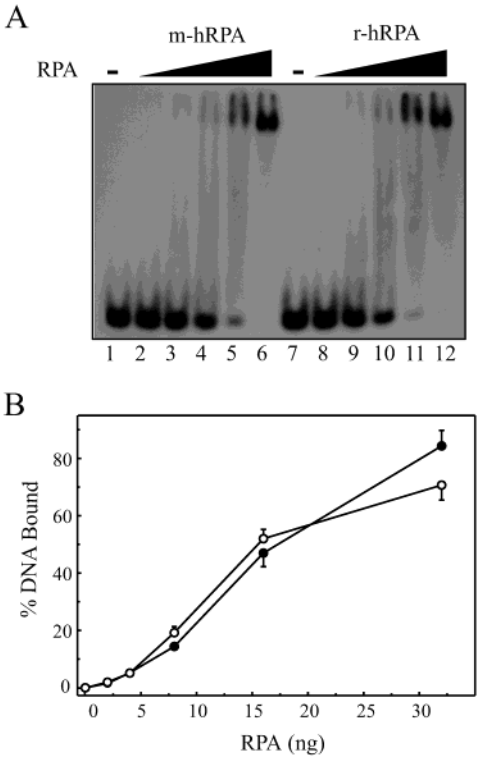

FIGURE 3: m-hRPA has similar ssDNA binding activity as r-hRPA. (A) EMSAs were carried out as previously described (*38*). Oligonucleotides were 5′-labeled with [γ-^{32}P]ATP using T4 kinase and purified as described in Materials and Methods. The indicated amounts of either m-hRPA or r-hRPA were incubated with 50 fmol of labeled oligo(dT_{30}) in a total volume of 20 μL. Following a 20 min incubation, RPA-p34 antibody (125 ng) was added to each sample for an additional 10 min. The products were separated on a 4% native polyacrylamide gel. Lanes 1 and 7 are free labeled oligo(dT_{30}) only; lanes 2−6 and 8−12 contain 2, 4, 8, 16, and 32 ng of m-hRPA and r-hRPA, respectively. (B) Quantification of the m-hRPA (filled circles) and r-hRPA (open circles) binding data from panel A is presented and represents the average of two individual experiments. Error bars correspond to the range of values. The equilibrium binding experiment was also performed in the absence of RPA antibody, and the relative binding activity of phosphorylated and unphosphorylated RPA was similar to that shown in Figure 3 (data not shown).

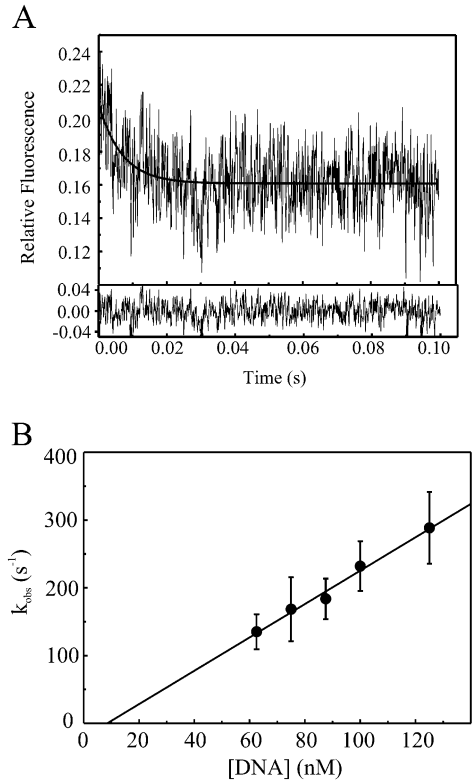

FIGURE 4: Stopped-flow kinetic analysis of m-hRPA binding ssDNA (dT_{30}). (A) The kinetic trace for m-hRPA binding to dT_{30} ssDNA. The trace was fit to a single-exponential decay (thick line), and the residual values for the fit are presented below the trace. Kinetic traces were measured at a constant m-hRPA concentration of 6.25 nM and varying DNA concentrations from 62.5 to 125 nM. Each trace used was an average of 8−10 measurements at each DNA concentration. (B) The k_{obs} values were plotted vs DNA concentration, and the linear fit provided the rate of association, k_{on}. Each point represents the average of two separate experiments, and the error bars correspond to the range of values.

difference in ssDNA binding between m-hRPA and r-hRPA. These data are consistent with phosphorylation playing no effect on RPA ssDNA binding.

Phosphorylation of RPA Inhibits DNA Binding to Undamaged and Cisplatin-Damaged dsDNA. RPA has previously been shown to preferentially bind cisplatin-damaged dsDNA versus undamaged dsDNA (*41*, *42*). To assess whether phosphorylation affects dsDNA binding, EMSAs were performed with m-hRPA and r-hRPA using 30-bp dsDNA substrates with and without a single 1,2 d(GpG) cisplatin lesion (Figure 5A). Increasing concentrations of either m-hRPA or r-hRPA were titrated into reactions containing undamaged or cisplatin-damaged dsDNA containing a single 1,2 d(GpG) adduct. Increasing RPA resulted in increasing RPA−DNA complex formation, although it is clear that the m-hRPA bound less DNA than the r-hRPA. The m-hRPA still displayed damage specificity in dsDNA binding, but compared to the r-hRPA, much less DNA was bound. Quantification of the results revealed approximately a 4−6-fold difference in dsDNA binding between the m-hRPA and the r-hRPA protein with the largest difference being with the undamaged dsDNA (Figure 5B, compare open circles with filled circles). Previously, it was shown that dsDNA binding of RPA correlated with its ability to denature the dsDNA strands (*34*). Interestingly, hyperphosphorylated RPA dsDNA binding also correlates with the denaturation of the dsDNA substrate (our unpublished data). These data suggest that phosphorylation affects how RPA binds to and destabilizes dsDNA. This could potentially be due to an alteration in the direct interaction of the p34 subunit with DNA or a change in the conformation of RPA complex leading to a change in DNA binding through the p70 subunit. The cisplatin-DNA adduct may distort the 30-bp dsDNA substrate giving it more single-stranded character, thereby reducing the distinction between the two forms of RPA. Interestingly, RPA purified from asynchronous HeLa cells (hRPA) still shows less dsDNA binding than r-hRPA but displays about 3-fold better binding to dsDNA than the m-hRPA (data not shown). It is possible that the hRPA protein purified from cycling cells is partially phosphorylated (potentially 1−2 phosphates). This would help explain the difference observed in dsDNA binding between r-hRPA, hRPA, and m-hRPA. Alternatively, the dsDNA binding activity observed with m-hRPA may be a result of the small amount of unphosphorylated Form 1 in the m-hRPA preparation.

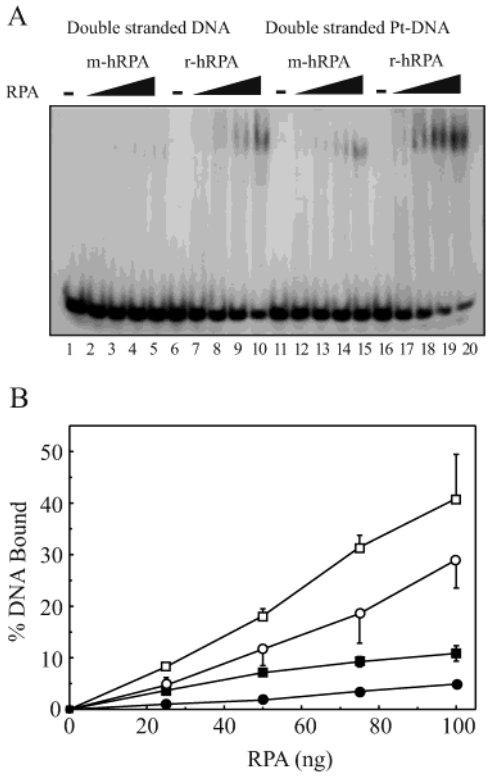

FIGURE 5: Phosphorylation of RPA inhibits DNA binding to undamaged and cisplatin-damaged dsDNA. EMSAs were carried out using 20 fmol of 30-bp undamaged dsDNA (lanes 1−10) or using the same 30-bp oligo containing a single 1,2d(GpG) cisplatin adduct (lanes 11−20). Lanes 1, 6, 11, and 16 without added m-hRPA or r-hRPA; lanes 2−5 and 12−15 contain 25, 50, 75, and 100 ng of m-hRPA; lanes 7−10 and 17−20 contain 25, 50, 75, and 100 ng of r-hRPA. The products were separated on a 4% native polyacrylamide gel. (B) Quantification of increasing concentrations of m-hRPA (filled circles) and r-hRPA (open circles) binding undamaged dsDNA and increasing concentrations of m-hRPA (filled squares) and r-hRPA (open squares) binding cisplatin damaged DNA. The data presented are the average of two individual experiments, and error bars correspond to the range of values.

RPA-p34 Phosphorylation Alters Protein−Protein Interaction In Vitro. Many proteins have been shown to interact with RPA, including the nucleotide excision repair protein XPA (*24*, *45*), the DNA replication protein DNA pol α (*26*), and the PI-3 kinase DNA-PK$_{cs}$ (*43*). In this study, we also demonstrate that purified ATM protein can bind to r-hRPA, and r-hRPA can be immunoprecipitated with an ATM antibody (Figure 6). The ATM protein and DNA-PK are thought to be responsible for the in vivo DNA damage-dependent phosphorylation of RPA (*14*, *16*, *44*−*46*). To assess whether phosphorylation plays a role in altering the RPA protein−protein interactions, we performed co-immunoprecipitation analyses comparing r-hRPA and m-hRPA with respect to interaction with the XPA protein, ATM, DNA-PK, and DNA pol α, respectively. Each purified protein (see Materials and Methods) was incubated with RPA and then precipitated with its own specific antibody, and both the supernatant (S) and the immunoprecipitate (P) were analyzed by Western blot analysis using the RPA-p34 antibody. Control experiments using r-hRPA and antibodies to XPA, ATM, DNA-PK, or DNA pol α without the interacting protein show no ability to pull down the RPA protein (data not shown). The results presented in Figure 6 demonstrate

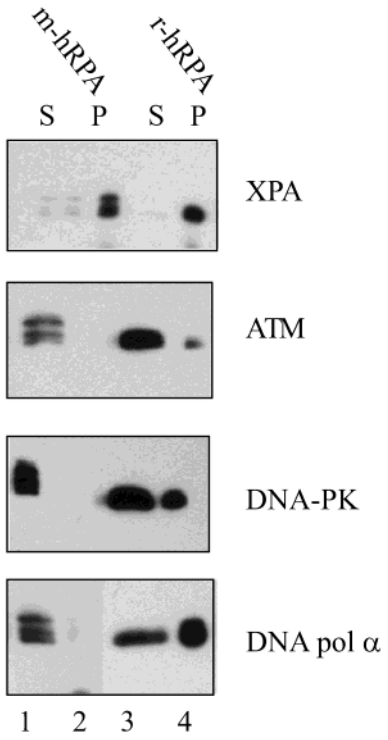

FIGURE 6: RPA-p34 phosphorylation alters protein−protein interaction in vitro. Purified m-hRPA or r-hRPA (100 ng) was mixed with purified XPA, ATM, DNA-PK, or DNA pol α (500 ng) for 30 min on ice. The mixture was incubated further with anti-XPA, ATM, DNA-PK, or DNA pol α overnight at 4 °C. The proteins were immunoprecipitated with protein G-agarose, and RPA-p34 was detected by Western blotting. Each panel is marked with the appropriate protein. Lanes 1 and 3 contain the supernatant separated by centrifugation (S) for m-hRPA or r-hRPA, respectively. Lanes 2 and 4 are the immunoprecipitate pellet (P) for m-hRPA and r-hRPA, respectively.

that the XPA protein efficiently interacts with both the m-hRPA (lane 2) and the r-hRPA protein (lane 4). These results demonstrate that RPA phosphorylation does not affect the interaction between the two proteins. The ATM protein interacts weakly with r-hRPA, and this interaction is abolished by phosphorylation as might be predicted for an enzyme/substrate interaction (lanes 2 and 4). DNA-PK interacts with the r-hRPA, but like the ATM protein, interaction is abolished by phosphorylation of RPA. DNA pol α also interacts with the r-hRPA protein, and like the ATM and DNA-PK proteins, phosphorylation disrupts the RPA-DNA pol α interaction (lanes 2 and 4). These data are consistent with the possibility that RPA phosphorylation in mitosis may inhibit DNA replication by disrupting or inhibiting the interaction with DNA pol α, while having no effect on the interaction with the XPA protein and thus having no effect on nucleotide excision repair.

Dephosphorylation of m-hRPA Restores Protein−Protein Interactions. To determine if the RPA phosphorylation effect was reversible, calf intestinal phosphatase (CIP) was used to dephosphorylate the m-hRPA, and the immunoprecipitation experiments were repeated (Figure 7). Treatment of m-hRPA with CIP resulted in a form of RPA that migrated similarly to the r-hRPA protein as determined by single dimension SDS−PAGE. The CIP-treated m-hRPA interacts to the same extent as untreated m-hRPA with XPA, as expected since no difference in the ability to interact with XPA was observed between the r-hRPA and the m-hRPA

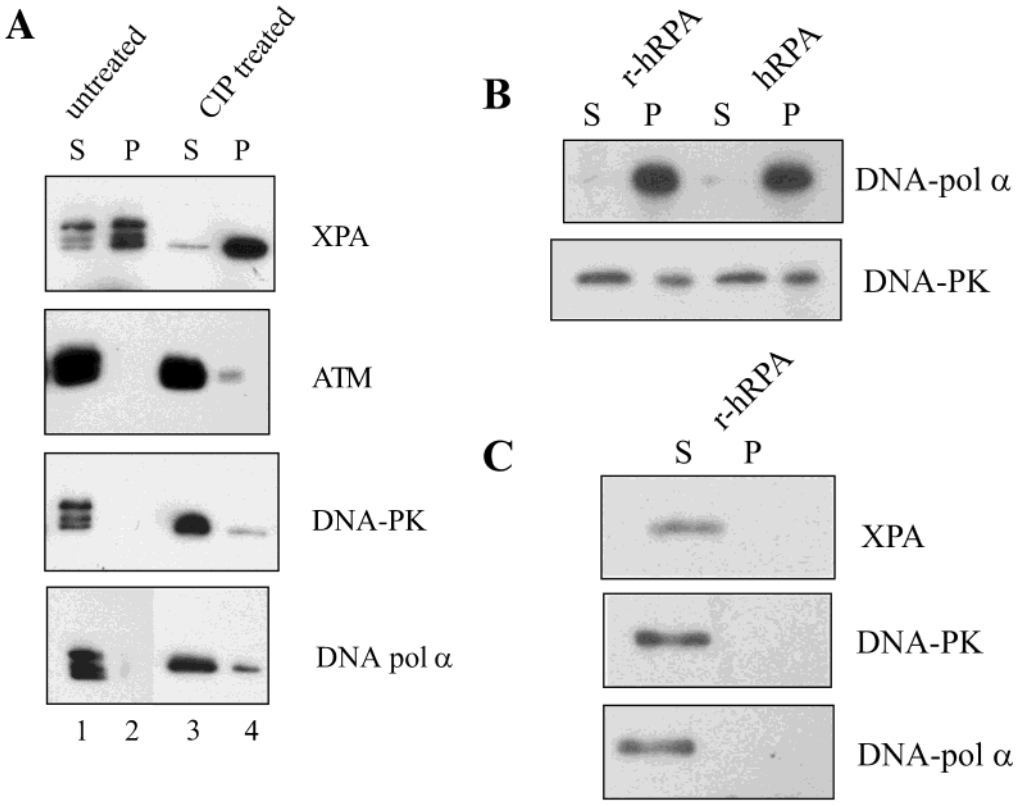

FIGURE 7: (A) Dephosphorylation of m-hRPA restores protein−protein interaction. Purified m-hRPA (100 ng) or CIP treated m-hRPA (100 ng) was mixed with XPA, ATM, DNA-PK, and DNA pol α. The products were incubated further with antibodies to the respective proteins and incubated overnight at 4 °C. After immunoprecipitation, RPA-p34 was detected by Western immunoblotting using anti-RPA-p34 monoclonal antibody. Lanes contain an equal volume of the supernatant (S) and the immunoprecipitates (P). Lanes 1 and 3 correspond to the supernatant for the untreated m-hRPA and CIP treated m-hRPA, respectively, while lanes 2 and 4 are the immunoprecipitate (P) for the untreated and CIP treated m-hRPA, respectively. (B) Purified r-hRPA or hRPA were combined with XPA, DNA-PK, and DNA pol α. Lanes 1 and 3 correspond to the supernatant (S) for the r-hRPA and hRPA, respectively, while lanes 2 and 4 are the immunoprecipitate (P) for the r-hRPA and hRPA, respectively. (C) Purified r-hRPA was combined with XPA, DNA-PK, or DNA pol α. The products were incubated further with the control IgG antibody and protein G-agarose. After immunoprecipitation, RPA-p34 was detected by Western immunoblotting using anti-RPA-p34 monoclonal antibody.

(Figure 6, lanes 2 and 4). Interestingly, different results were obtained assessing the interaction of CIP-treated m-hRPA with ATM. In the absence of CIP, the m-hRPA showed very little interaction with ATM (as shown in Figure 6). CIP treatment of m-hRPA resulted in an increased interaction with the ATM protein that was not observed in mock-dephosphorylated m-hRPA (Figure 7A, compare lanes 2 and 4). In addition, both the DNA-PK− and the DNA pol α−RPA interactions were partially recovered by CIP treatment (Figure 7A, lanes 2 and 4). Quantification of the data reveals that CIP treatment of m-hRPA restored binding to ATM, DNA-PK, and DNA pol α to levels that were 77, 15, and 33% of the r-hRPA binding, respectively. However, more importantly, the increase in protein binding observed with CIP-treated m-hRPA was 25, 15, and 13.5-fold above the very low but measurable levels observed with untreated phosphorylated m-hRPA binding to ATM, DNA-PK, and DNA pol α, respectively. Clearly, this is a significant and specific increase as no binding was observed above the background for the nonspecific IgG control. To validate the differences observed in protein binding between m-hRPA and r-hRPA control, in vitro binding experiments comparing purified hRPA and r-hRPA were carried out. The protein−protein interactions between hRPA and XPA DNA-PK and DNA pol α were similar to r-hRPA (data not shown and Figure 7B). In addition, control experiments using r-hRPA and nonspecific IgG antibody to confirm the specificity of the interactions show no ability to pull down the RPA protein (Figure 7C). The inability to recover 100% of the protein−protein interactions by CIP treatment of m-hRPA could be a result of numerous factors including the processing of samples for treatment with CIP. The fact that no interaction is detected with the m-hRPA and upon dephosphorylation, a clear, specific interaction is regained strongly suggest that phosphorylation plays a major role in RPA−protein interactions, which ultimately may affect the regulation of the biological functions of RPA.

DISCUSSION

We have investigated the functional consequences of the RPA-p34 phosphorylation that is associated with the mitotic phase of the cell cycle. In normally cycling cells, RPA-p34 exists in three forms: one unphosphorylated and two different phosphorylated forms. We have purified and characterized one of these forms of RPA, which is specifically associated with the mitotic phase of the cell cycle. We have used purified m-hRPA to show that binding affinity for undamaged and cisplatin-damaged dsDNA is reduced as compared with r-hRPA; however, ssDNA binding affinity is unchanged. Furthermore, purified phosphorylated m-hRPA exhibited decreased association with purified DNA pol α and DNA-PK. RPA/XPA interaction was unaffected by RPA

phosphorylation. We also discovered that purified r-hRPA interacts directly with purified ATM in vitro, and this interaction is absent with m-hRPA. This observation is consistent with the observation that RPA and ATM co-localize on meiotic chromatin (*47*). We conclude that the phosphorylation of RPA-p34 alters specific protein−protein interactions and dsDNA binding activity.

It has been postulated that the ability of RPA to bind to double-stranded DNA is a reflection of its capacity to cause unwinding of dsDNA. This unwinding activity does not require ATP and does not reflect helicase activity but rather a helix-destabilizing activity. The unwinding activity of RPA appears to require thermally unstable sequences and is more pronounced with damaged DNA such as the cisplatin-containing dsDNA used here. We observed that the binding affinity of the phosphorylated m-hRPA was the same as that of the unphosphorylated r-hRPA to ssDNA. In contrast, the binding to both damaged and undamaged dsDNA was reduced 4−6-fold in m-hRPA. Interestingly, calf thymus RPA phosphorylated in vitro using chicken cdc2 kinase resulted in an increase in DNA unwinding (*48*). In vitro, the cdc2 kinases appear to phosphorylate RPA-p34 primarily at serine 29, characteristic of the S-phase form (Form 2) of RPA. The mitotic form we have used is phosphorylated on at least two sites (*10*). If binding to dsDNA indeed reflects DNA unwinding activity, then both our observations are consistent with phosphorylation modulating the DNA unwinding activity of RPA. The direction of the modulation would then be specific for the differentially phosphorylated forms of RPA. Alternatively, binding to dsDNA may reflect RPA activities that are distinct from DNA unwinding. One might speculate that in S-phase, DNA unwinding is important in the DNA replication function of RPA, while in mitosis, RPA may be required to participate in protein−protein interactions that promote DNA stability.

RPA has been shown to interact with a number of proteins involved in DNA replication and DNA repair. In particular, it was shown previously that purified human RPA bound specifically to purified human DNA pol α (*26*). Here we show that unphosphorylated r-hRPA associates in vitro with DNA pol α, whereas no association between purified m-hRPA and DNA pol α could be detected by co-immunoprecipitation. Similarly, Wold and colleagues (personal communication) have found that r-hRPA with multiple serine to aspartic acid substitutions in the N-terminal region of RPA-p34 also exhibits reduced affinity for DNA pol α.

The results presented here demonstrate that the interaction between purified RPA and purified DNA-PK in vitro is altered by RPA-p34 phosphorylation. RPA has previously been shown to bind to DNA-PK_{cs} in vitro, and the RPA-p70 subunit was required for the efficient interaction of the two proteins (*22*). A possible role for RPA-p34 phosphorylation in protein−protein interaction between RPA and DNA-PK was suggested by the observation that association between RPA and DNA-PK in cells was disrupted after camptothecin-induced DNA damage (*22*), which results in hyperphosphorylation of RPA. The results presented here involve a direct role for phosphorylation in protein−protein interaction in vitro between RPA and DNA-PK. In addition, we show here for the first time that unphosphorylated RPA forms a complex with ATM in vitro, and this interaction is eliminated by phosphorylation as might be predicted for an enzyme/substrate interaction. Furthermore, RPA interacted with ATM in untreated HeLa cells (data not shown). We have previously shown that RPA is hyperphosphorylated by ATM and DNA-PK in vitro, and many of the sites phosphorylated in vivo are identical to those identified in vitro *(10, 14)*. An interesting hypothesis is that ATM and/or DNA-PK catalyzed phosphorylation of RPA act as a molecular switch to redirect RPA from the replication complex to interact with proteins involved in DNA recombination or repair.

Cell-cycle-dependent phosphorylation of RPA was first reported by Din et al. and was shown to occur at serines 23 and 29 of RPA-p34 (*4, 8*). Cyclin B/$p34^{cdc2}$ phosphorylates these sites in vitro. The phosphorylation observed at the onset of S-phase (Form 2) appears to be independent of DNA replication and elongation (*14, 49*). In addition, a double mutant strain of *S. cerevisiae*, incapable of replicating DNA but continuing through the cell cycle, is proficient in the primary phosphorylation of Rfa2 (*16, 44*). A biological role for S-phase related phosphorylation has not been demonstrated; however, the requirement for RPA in the initiation of DNA replication and its phosphorylation in a cell-cycle-dependent manner makes it a likely candidate to play a key role in regulating DNA replication. In xenopus cell-free extracts, S-phase phosphorylation of RPA-p34 is dependent on association with DNA, whereas mitotic phosphorylation of RPA is independent of DNA binding (*50*). Similarly, DNA-PK- and ATM-catalyzed in vitro phosphorylation of RPA-p34 is dependent on ssDNA, whereas cyclin B/$p34^{cdc2}$ catalyzed in vitro phosphorylation does not require DNA (*14*). During embryogenesis in *Drosophila melanogaster*, the phosphorylated form of RPA-p30 is tightly regulated and most abundant during mitosis. Separation by two-dimensional gel electrophoresis resolved the mitotic form into two major species with similar molecular weight that differed mainly by charge (*51*). It will be important to determine the exact sites of phosphorylation of the various cell-cycle forms and to determine the kinases responsible.

NMR analysis has revealed that the N-terminus of RPA-p34, containing the phosphorylation sites, acts independently of the heterotrimer core complex (*32*). The unrestricted motion of the N-terminus along with the phosphorylation of specific serine and threonine residues could alter the heterotrimer conformation making it unfavorable for certain protein−protein interactions, while favoring others. We have categorized the phosphorylated forms of RPA-p34 into four distinct forms, Forms 2−5, according to their electrophoretic mobility in one dimension. It is possible that each band could be made up of multiple phosphorylated forms with an equal number of phosphorylated residues but located at different sites within the N-terminus. This could give rise to different forms that act preferentially in replication, repair, or recombination. RPA is known to interact with the recombinational repair protein Rad52 via the N-terminus of the p70 and the C-terminus of the p34 subunits (*32, 51, 52*). Indeed, it is inviting to speculate that mitotic-specific phosphorylation may decrease interactions with other DNA replication proteins such as DNA pol α, redirecting the RPA tasks in the direction of recombinational repair. Genetic analysis in *S. cerevisiae* provides additional evidence that RPA is a key element in mitotic recombination processes and interacts with Rad52 (*53*). Further evidence that RPA is involved in double

strand break repair is demonstrated by increased DSB-induced deletions and translocations observed in the mutation spectrum of mutant alleles of the p70 subunit (*54*). It is interesting that the interaction of XPA with RPA is unaffected by phosphorylation of the p34 subunit. This insensitivity may reflect the importance of having a functional NER complex independent of the phase of the cell cycle. These results are also consistent with reports of the insensitivity of in vitro catalyzed NER to the state of RPA phosphorylation (*17*).

In summary, we have demonstrated that cell-cycle-dependent phosphorylation of RPA-p34 in mitosis decreases double-stranded DNA binding activity and alters protein−protein interaction. We postulate that phosphorylation of RPA acts as a molecular switch to control the role of RPA in multiple pathways of DNA metabolism. Further, we suggest that phosphorylation of the p34 subunit induces subtle conformational changes that influence the ability of RPA to interact with other proteins and bind DNA.

REFERENCES

1. Wold, M. S. (1997) *Annu. Rev. Biochem. 66*, 61−92.
2. Iftode, C., and Borowiec, J. A. (1997) *Mol. Cell Biol. 17*, 3876−3883.
3. Iftode, C., Daniely, Y., and Borowiec, J. A. (1999) *Crit. Rev. Biochem. Mol. Biol. 34*, 141−180.
4. Din, S., Brill, S. J., Fairman, M. P., and Stillman, B. (1990) *Genes Dev. 4*, 968−977.
5. Fotedar, R., and Roberts, J. M. (1992) *EMBO J. 11*, 2177−2187.
6. Dutta, A., and Stillman, B. (1992) *EMBO J. 11*, 2189−2199.
7. Pan, Z. Q., Amin, A. A., Gibbs, E., Niu, H., and Hurwitz, J. (1994) *Proc. Natl. Acad. Sci. U.S.A. 91*, 8343−8347.
8. Niu, H., Erdjument-Bromage, H., Pan, Z. Q., Lee, S. H., Tempst, P., and Hurwitz, J. (1997) *J. Biol. Chem. 272*, 12634−12641.
9. Henricksen, L. A., and Wold, M. S. (1994) *J. Biol. Chem. 269*, 24203−24208.
10. Zernik-Kobak, M., Vasunia, K., Connelly, M., Anderson, C. W., and Dixon, K. (1997) *J. Biol. Chem. 272*, 23896−23904.
11. Carty, M. P., Zernik-Kobak, M., McGrath, S., and Dixon, K. (1994) *EMBO J. 13*, 2114−2123.
12. Liu, V. F., and Weaver, D. T. (1993) *Mol. Cell Biol. 13*, 7222−7231.
13. Gately, D. P., Hittle, J. C., Chan, G. K., and Yen, T. J. (1998) *Mol. Biol. Cell 9*, 2361−2374.
14. Oakley, G. G., Loberg, L. I., Yao, J. Q., Risinger, M. A., Yunker, R. L., Zernik-Kobak, M., Khanna, K. K., Lavin, M. F., Carty, M. P., and Dixon, K. (2001) *Mol. Biol. Cell 12*, 1199−1213.
15. Wang, H., Guan, J., Wang, H., Perrault, A. R., Wang, Y., and Iliakis, G. (2001) *Cancer Res. 61*, 8554−8563.
16. Brush, G. S., Anderson, C. W., and Kelly, T. J. (1994) *Proc. Natl. Acad. Sci. U.S.A. 91*, 12520−12524.
17. Pan, Z. Q., Park, C. H., Amin, A. A., Hurwitz, J., and Sancar, A. (1995) *Proc. Natl. Acad. Sci. U.S.A. 92*, 4636−4640.
18. Lee, S. H., and Kim, D. K. (1995) *J. Biol. Chem. 270*, 12801−12807.
19. Ariza, R. R., Keyse, S. M., Moggs, J. G., and Wood, R. D. (1996) *Nucleic Acids Res. 24*, 433−440.
20. Morgan, S. E., and Kastan, M. B. (1997) *Cancer Res. 57*, 3386−3389.
21. Liu, J. S., Kuo, S. R., McHugh, M. M., Beerman, T. A., and Melendy, T. (2000) *J. Biol. Chem. 275*, 1391−1397.
22. Shao, R., Cao, C., Zhang, H., Kohn, K., Wold, M., and Pommier, Y. (1999) *EMBO J. 18*, 1397−1406.
23. Dutta, A., Ruppert, J. M., Aster, J. C., and Winchester, E. (1993) *Nature 365*, 79−82.
24. Matsuda, T., Saijo, M., Kuraoka, I., Kobayashi, T., Nakatsu, Y., Nagai, A., Enjoji, T., Masutani, C., Sugasawa, K., Hanaoka, F., Yasui, A., and Tanaka, K. (1995) *J. Biol. Chem. 270*, 4152−4157.
25. He, Z., Brinton, B. T., Greenblatt, J., Hassell, J. A., and Ingles, C. J. (1993) *Cell 73*, 1223−1232.
26. Braun, K. A., Lao, Y., He, Z., Ingles, C. J., and Wold, M. S. (1997) *Biochemistry 36*, 8443−8454.
27. Miller, S. D., Moses, K., Jayaraman, L., and Prives, C. (1997) *Mol. Cell Biol. 17*, 2194−2201.
28. Golub, E., Gupta, R., Haaf, T., Wold, M., and Radding, C. (1998) *Nucleic Acids Res. 26*, 5388−5393.
29. Stigger, E., Drissi, R., and Lee, S. H. (1998) *J. Biol. Chem. 273*, 9337−9343.
30. Loor, G., Zhang, S. J., Zhang, P., Toomey, N. L., and Lee, M. Y. (1997) *Nucleic Acids Res. 25*, 5041−5046.
31. New, J. H., Sugiyama, T., Zaitseva, E., and Kowalczykowski, S. C. (1998) *Nature 391*, 407−410.
32. Mer, G., Bochkarev, A., Gupta, R., Bochkareva, E., Frappier, L., Ingles, C. J., Edwards, A. M., and Chazin, W. J. (2000) *Cell 103*, 449−456.
33. Abramova, N. A., Russell, J., Botchan, M., and Li, R. (1997) *Proc. Natl. Acad. Sci. U.S.A. 94*, 7186−7191.
34. Patrick, S. M., and Turchi, J. J. (1999) *J. Biol. Chem. 274*, 14972−14978.
35. Patrick, S. M., and Turchi, J. J. (2001) *J. Biol. Chem. 276*, 22630−22637.
36. Hermanson, I. L., and Turchi, J. J. (2000) *Prot. Express. Purif. 19*, 1−11.
37. Reveal, P. M., Henkels, K., Turchi, J. J., and Henkels, K. (1997) *J. Biol. Chem. 272*, 11678−11681.
38. Turchi, J. J., and Henkels, K. (1996) *J. Biol. Chem. 271*, 13861−13867.
39. Henkels, K. M., and Turchi, J. J. (1997) *Cancer Res. 57*, 4488−4492.
40. Johnson, R. T., Collins, A. R., Squires, S., Mullinger, A. M., Elliott, G. C., Downes, C. S., and Rasko, I. (1987) *J. Cell Sci. Suppl. 6*, 263−288.
41. Patrick, S. M., and Turchi, J. J. (1998) *Biochemistry 37*, 8808−8815.
42. Clugston, C. K., McLaughlin, K., Kenny, M. K., and Brown, R. (1992) *Cancer Res. 52*, 6375−6379.
43. Anderson, C. W., and Lees-Miller, S. P. (1992) *Crit. Rev. Eukaryotic Gene Express. 2*, 283−314.
44. Brush, G. S., Morrow, D. M., Hieter, P., and Kelly, T. J. (1996) *Proc. Natl. Acad. Sci. U.S.A. 93*, 15075−15080.
45. Cheng, X., Cheong, N., Wang, Y., and Iliakis, G. (1996) *Radiother. Oncol. 39*, 43−52.
46. Henricksen, L. A., Carter, T., Dutta, A., and Wold, M. S. (1996) *Nucleic Acids Res. 24*, 3107−3112.
47. Plug, A., Peters, A., Xu, Y., Keegan, K., Hoekstra, M., Baltimore, D., de, B. P., and Ashley, T. (1997) *Nat. Genet. 17*, 457−461.
48. Georgaki, A., and Hubscher, U. (1993) *Nucleic Acids Res. 21*, 3659−3665.
49. Rodrigo, G., Roumagnac, S., Wold, M., Salles, B., and Calsou, P. (2000) *Mol. Cell Biol. 20*, 2696−2705.
50. Fang, F., and Newport, J. W. (1993) *J. Cell Sci. 106*, 983−994.
51. Mitsis, P. G. (1995) *Dev. Biol. 170*, 445−456.
52. Hays, S. L., Firmenich, A. A., Massey, P., Banerjee, R., and Berg, P. (1998) *Mol. Cell Biol. 18*, 4400−4406.
53. Firmenich, A. A., Elias-Arnanz, M., and Berg, P. (1995) *Mol. Cell Biol. 15*, 1620−1631.
54. Chen, C., and Kolodner, R. D. (1999) *Nat. Genetics 23*, 81−85.

BI026377U